Cryogenics 136 (2023) 103756

Contents lists available at ScienceDirect

Cryogenics

journal homepage: www.elsevier.com/locate/cryogenics

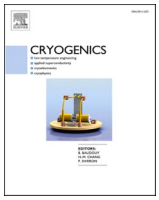

Non-magnetic regenerator material of silver oxide for 4 K cryocoolers

Sotaro Nishioka [a,*], Shinji Masuyama [b], Akiko T. Saito [a]

[a] National Institute for Materials Science, Ibaraki 305-0003, Japan
[b] Department of Electronic-Mechanical Engineering, National Institute of Technology, Oshima College, Yamaguchi 742-2193, Japan

ARTICLE INFO

Keywords:
Regenerator material
Optical phonon
Cryocooler

ABSTRACT

In regenerative cryocoolers, magnetic specific heat is often utilized for heat regeneration at cryogenic temperature, such as below 20 K. Magnetic regenerator materials of rare earth compound which have sufficient specific heat enabled cryocooler to reach below 4 K. However, the magnetic noise emitted from the magnetic materials during the refrigeration cycle affects the performance of noise-sensitive devices. In this study, we propose a non-magnetic regenerator material having "optical phonon degree of freedom" even at cryogenic temperatures, in which silver oxide (Ag_2O) is selected. Ag_2O decomposes at temperature above 410 K in ambient atmosphere, whereas we succeeded in fabricating a sintered Ag_2O bulk and small particles of the size of 0.5 mm with high-density more than 90%. Specific heat measurement down to 100 mK was performed for the sintered bulk sample of Ag_2O. Below 10 K, a non-Debye behavior was observed, suggesting the contribution from optical phonon modes. Calculation of the phonon density of state (phDOS) performed by the Evolution Strategy algorithm in addition to the first-principles calculation reveals that phDOS has several distinct peaks at low energies, and the low-energy optical phonons contribute to the non-Debye behavior. The low temperature specific heat of Ag_2O enhanced by the optical phonons is larger than conventional non-magnetic regenerator materials when compared in terms of specific heat per volume. Moreover, the calculation of cooling performance of cryocooler using Ag_2O particles is found to be reached below 4.2 K. This study shows that non-magnetic material with low temperature specific heat enhanced by optical phonon mode can be used as a regenerator material for regenerative cryocoolers.

1. Introduction

Recently, there is a growing interest in application of various types of regenerative cryocooler for quantum computers, superconducting magnets and other cryogenic devices. Among these regenerative cryocoolers, a Gifford-McMahon (GM) cryocooler is comparatively popular and well adopted in various fields. It is designed in the form of multi-stage cooling process to generate a large temperature difference from room temperature (R.T.) to cryogenic temperature. Various regenerator materials, which possess large specific heats under set operating temperatures, are used in both 1st cooling stage and 2nd cooling stage. For example, lead (Pb) and bismuth (Bi) are often used as regenerator materials in the 2nd cooling stage. This is because their Debye temperatures θ_D = 105 K and 119 K, respectively, are relatively lower than other materials and yet possess large specific heat even at low temperatures. However, as this specific heat produced from the acoustic phonon degree of freedom in accordance with the Debye behavior decreases substantially T^3 law in temperature ($T \ll \theta_D$). Therefore, the lowest temperature attained by cryocooler using these materials can only go down to lowest ~ 5 K. A new regenerator material was introduced in 1980 s', where magnetic specific heat was produced from the electron spin degree of freedom to improve the cooling performance [1–3]. The operating temperature can then go down to as low as 2 K and condensation of He gas has become possible. Currently, regenerator applying both magnetic materials (such as $HoCu_2$ and Gd_2O_2S) and non-magnetic materials such as Bi, is commonly used to achieve the cryogenic temperatures [4,5]. However, there is a setback when using the magnetic regenerator material in which emission of its magnetic noise affects the measurement sensitivity in equipment such as magnetospinography [6], magnetic resonance imaging (MRI) and quantum computer. For this reason, it is desired to develop a magnetic noise free material. We focus on specific heat produced from the "optical phonon degree of freedom" and a non-magnetic material Ag_2O was selected [7]. The crystal structure of Ag_2O is a cubic cuprite type with a space group of *Pn-3 m* (Fig. 1). From the previous studies, it is known that the anharmonic optical phonon mode bends the O-Ag-O link, which is on a straight line in

* Corresponding author.
E-mail address: NISHIOKA.Sotaro@nims.go.jp (S. Nishioka).

https://doi.org/10.1016/j.cryogenics.2023.103756
Received 17 August 2023; Received in revised form 28 September 2023; Accepted 10 October 2023
Available online 12 October 2023

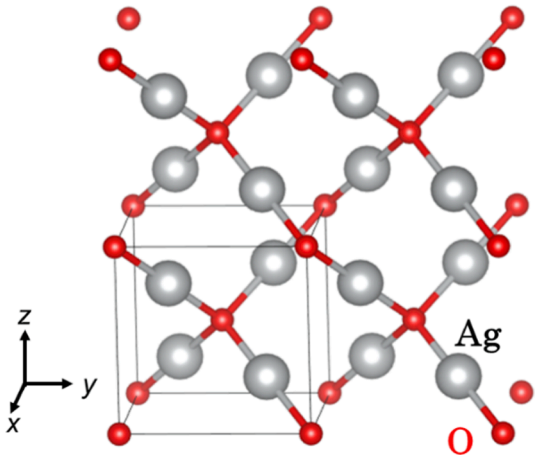

Fig. 1. The crystal structure of Ag_2O is of cubic cuprite type (space group of *Pn-3 m*). The Ag_2O has a linear O-Ag-O link.

ground state [8,9]. The Ag atom with a relative heavy mass, contributes to optical phonon modes at low energies leading to a non-Debye specific heat at low temperatures [10,11]. The regenerator material for GM cryocooler should possess a large specific heat and to be of spherical shape with a size in submillimeter. When forming a spherical particle of Ag_2O, special handling is required to avoid decomposition of Ag_2O into silver and oxygen above 410 K in ambient atmosphere [12,13].

In this paper, we report the spheroidization of Ag_2O in submillimeter and the result of specific heat measurement of Ag_2O down to 100 mK. The temperature dependence of specific heat below 10 K exhibits a non-Debye behavior, suggesting contribution of optical phonon even in at low temperatures. At cryogenic temperature, the Ag_2O exhibits a substantially larger volumetric specific heat than conventional non-magnetic regenerator materials such as Pb and Bi. Moreover, we also succeeded in applying a unique mold sintering to fabricate a spherical particle with a high-density of more than 90% and a diameter of 0.5 mm. Besides, in addition to the first-principles calculation, the Evolution Strategy (ES) algorithm was applied to calculate phDOS from the specific heat measurement data. It is found that phDOS has several distinct peaks at low energies, and these low-energy optical phonons contribute to the non-Debye behavior.

2. Experiments

2.1. Preparation method of bulk and spherical sample of Ag_2O

Raw material Ag_2O which is in powder form, of purity greater than 99%, was sintered using the spark plasma sintering (SPS) at 40 MPa at 623 K under vacuum condition for 15 min. The X-ray diffraction (XRD) patterns of both raw material and the sintered bulk sample of Ag_2O were measured by using Cu Kα radiation source in the 2θ range from 10 to 80°. The XRD patterns shown in Fig. 2 (a) and (b) indicate that both samples have the same cuprite structures. Specific heat of Ag_2O bulk sample was measured at temperature from 100 mK to 300 K, by using the Physical Properties Measurement System (PPMS by Quantum Design, Inc.).

Spheroidization of Ag_2O was performed using three techniques. The first technique used a cross-linking reaction between sodium alginate $(NaC_6H_7O_6)_n$ (300 cps) and calcium lactate $C_6H_{10}CaO_6{\cdot}5H_2O$. In the spheroidization process, the powdery raw material of Ag_2O was mixed evenly with the sodium alginate solution (1 wt%) in a mass proportion of 6:10. The mixture was then injected through a syringe into the calcium lactate solution (5 wt%) to form a spherical Ag_2O (Sol-Gel technique). This continued with the drying process for the spherical Ag_2O in which it was drained and dried in ambient atmosphere. The second technique employed the pseudo isotropic pressure application for the purpose of

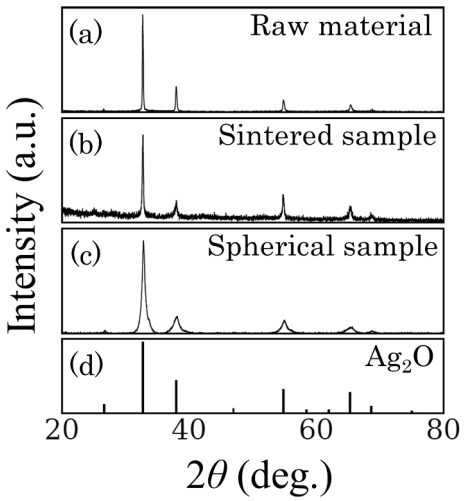

Fig. 2. XRD results of the respective Ag_2O samples (a) raw material, (b) sintered sample by SPS method and (c) spherical sample by mold sintering technique. (d) Calculated XRD pattern of Ag_2O. All these three XRD results display consistent peak patterns with that of the calculated XRD pattern shown in (d).

increasing the bulk density. After the spherical Ag_2O was fully dried under the first technique, it was then put in a pool of zirconia fine particles with diameter of ~ 30 μm and pressed at 40 MPa at 623 K in a vacuum condition for 15 min (pseudo isotropic pressing technique). The last technique was to apply direct hot press sintering to the powdery raw material of Ag_2O at 40 MPa at 623 K in a vacuum condition for 15 min (mold sintering technique). The spherical Ag_2O was fabricated by using multiple hemispherical microfabricated mold. The mold was pre-coated with a BN release agent for easy removal after the spheroidization process. All three kinds of spherical Ag_2O were confirmed to have the same cuprite structures by the XRD measurement. The XRD pattern of Ag_2O spherical particles prepared by mold sintering technique is shown in Fig. 2 (c). The peak pattern is identical to that of the raw material and the sintered bulk material as shown in Fig. 2 (a) and (b) respectively. This shows that this pattern corresponds to the single phase of Ag_2O with the cuprite structures. Meanwhile, the width of the XRD peak of the spherical particle is wider than those of other samples. This could be caused by microstructural strain or change in crystallite size after the fabrication process. Moreover, all three kinds of spherical Ag_2O particles were then analyzed using the X-ray micro computed tomography scan (TDM1601-II) in order to investigate filling structure within the particle.

2.2. Computational details

Cooling power of 4 K cryocooler with a 2nd cooling stage capacity of 1 W using Ag_2O as a regenerator material was calculated at temperature from 4.2 K to 8 K, by REGEN3.3 packages [14]. The typical input

Table 1
Input parameters for calculation using REGEN3.3.

Parameter	Value
Diameter of particle (mm)	0.5
Diameter of regenerator (mm)	35
Length of regenerator (mm)	140
Hot end temperature of 2nd stage (K)	50
Cold end temperature of 2nd stage (K)	4.2 – 8.0
Frequency (Hz)	1.2
Mass flux at the cold end (g/s)	4.5 – 6.0
Average pressure (MPa)	1.5
Pressure ratio at the cold end	3.2
Thermal conductivity of Ag_2O (W/K •m)	0.17 (5 K), 0.31 (10 K), 0.45 (15 K), 0.54 (20 K), 0.93 (40 K), 1.3 (60 K)

parameters for the calculation are listed in Table 1, in which several values are set based on reference from previous study [15].

The phDOS were calculated using two different methods, the first-principles calculation by using the Quantum-ESPRESSO and ALAMODE package, and the Covariance Matrix Adaptation Evolution Strategy (CMA-ES) [16–18]. First-principles calculation were performed with the generalized gradient approximation of density functional theory formulated by the Perdew, Burke, and Ernzerhof [19]. The Norm-Conserving (NC) and Projector-Augmented Wave (PAW) pseudopotentials in standard solid-state pseudopotential libraries (SSSP) were used for Ag and O, respectively [20–24]. Wave function cutoff of 80 Ry and charge density cutoff of 700 Ry were used. The Brillouin zone integrations were performed using Monkhorst-Pack grid of k-points 10 × 10 × 10. The interatomic force constants based on the supercell (2 × 2 × 2) approach have been calculated by ALAMODE package. The lattice parameter value is 4.811 Å at 0 K in this calculation, while the experimental value at 14 K is 4.745 Å [25]. The CMA-ES is an optimization algorism that derives an optimum solution even under the presence of multiple local minima, unlike the standard least-square methods. In this paper, this method was used to solve an inverse problem of obtaining phDOS from the specific heat measurement data.

3. Results and discussion

3.1. Specific heat and calculated phDOS

Fig. 3 shows the temperature dependence of volumetric specific heat C (J/cm^3 K) of the sintered Ag_2O (red dots) and conventional non-magnetic regenerator materials of Pb (blue dash-dotted line) [26] and Bi (black dotted line) [27]. The temperature dependence of specific heat of Ag_2O shows a linear behavior above 2 K, which relates to the non-Debye behavior caused by optical phonons [8]. The specific heat of Ag_2O reaches 6 times larger than that of Pb at 4.2 K, indicating that Ag_2O has a higher advantage as a regenerator material.

In order to investigate the origin of the non-Debye behavior of Ag_2O, we calculated the phDOS of Ag_2O using both ES method and first-principles calculation. Fig. 4(a) and 4(b) show the experimental results and calculations of both temperature dependences of specific heat and phDOS for Ag_2O, respectively. The red and the black solid lines in Fig. 4(a) represent the calculated results by the ES method and the first-principles calculation, respectively. The relation between specific heat $C_v(T)$ and phDOS $D(E)$ is expressed as

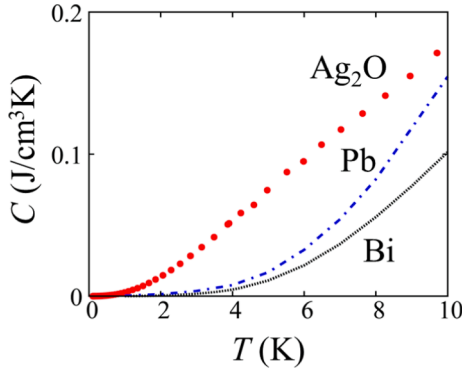

Fig. 3. Temperature dependence of volumetric specific heat C (J/cm^{3}K) of the sintered Ag_2O (red dots), conventional non-magnetic regenerator materials of Pb (blue dash-dotted line) [26] and Bi (black dotted line) [27]. Ag_2O has a larger specific heat than Pb and Bi at cryogenic temperature. The temperature dependence of specific heat of Ag_2O shows a linear behavior due to its optical phonon (non-Debye behavior). (For interpretation of the references to colour in this figure legend, the reader is referred to the web version of this article.)

$$C_v(T) = 9N_A k_B \int_0^\infty D(E) \frac{(\beta E)^2 e^{\beta E}}{(e^{\beta E} - 1)^2} dE, \quad (1)$$

where $\beta = 1/k_BT$, k_B is Boltzmann constant, N_A is Avogadro constant. The ES method were repeated until the obtained phDOS reproduced the specific heat measurement. As shown in Fig. 4(b), the results from both ES method and first-principles calculation show similar phonon spectra. It is characterized by the peaks at two regions, that is, one is around 10 meV and the other one is around 60 meV. This is also shown in the result of inelastic neutron scattering measurement at 40 K [9]. Similar spectra were also reported in previous studies [8,11,28,29]. Accuracy of the phonon spectrum calculated by the ES method at low energy region below 10 meV is considered high as it is calculated to fit to the specific heat measurement. On the other hand, the region of around 60 meV, the spectrum of the ES method is different from that of inelastic neutron scattering measurement as shown in Fig. 4(b). This would be due to the absent of specific heat data in the high temperature region (~ 60 meV). Therefore, in this case, we think that the ES method provide accurate phonon spectra around 10 meV, but the first-principles calculation calculates more accurate for around 60 meV.

3.2. Material spheroidization and calculated cooling performance

In order to put Ag_2O in practical use as a regenerator material, a high-density particle is necessary. Sintering method is often used to fabricate high-density sample in the field of powder metallurgy. However, it is difficult to sinter Ag_2O because it decomposes into silver and oxygen at temperature above 410 K in ambient atmosphere. Therefore, we have tried different approaches in order to obtain the high-density particle. Two types of photographs of each fabricated particle were taken under the optical microscopy in Fig. 5(a)-5(c) and X-ray micro computed tomography (micro-CT) in Fig. 5(d)-5(f). Fig. 5(a) and 5(d) show spherical Ag_2O made by the Sol-Gel technique, the spherical Ag_2O has a diameter of 2.0 mm and a bulk density of ~ 25%. The bulk density is calculated based on a true density of 7.22 g/cm^3 for Ag_2O. Since the bulk density of the Ag_2O sphere is rather low, the second technique, the pseudo isotropic pressing technique, was applied to continue the spheroidization process. As shown in Fig. 5(b) and 5(e), the sphere then shrunk further to a diameter of 1.5 mm and the bulk density increased to ~ 55%. Although the bulk density of Ag_2O sphere has increased, it is still not an ideal bulk density to be used as a practical regenerator material. Furthermore, zirconia particles also remained on the surface of the Ag_2O sphere as shown in Fig. 5(b). To further increase the bulk density, a unique mold sintering technique was employed. We succeeded in fabricating the Ag_2O spherical particle with a diameter of 0.5 mm and a bulk density of more than 90% (Fig. 5(c) and 5(f)). In addition to that, a thin layer of silver (Fig. 5(c)) formed on the surface of Ag_2O after the fabrication was found. The existence of the thin silver would increase the abrasion resistance against vibration occurred during the cryocooler operation.

Since we have succeeded in fabricating the Ag_2O particle with an ideal density as a practical regenerator material, we then utilized the properties of the Ag_2O particle to calculate the cooling power of the 2nd stage in GM cryocooler between 4.2 K and 8 K. For comparison purpose, the cooling power using the conventional non-magnetic regenerator materials Pb and Bi were also calculated. In the calculation, the diameter of particle of these materials is fixed at 0.5 mm. Fig. 6 shows calculated cooling power for Ag_2O, Pb and Bi particles used in the cryocooler at different temperatures. For Ag_2O particles, the cooling power remains even at 4.2 K. On the other hand, for Pb and Bi particles, their lowest temperatures can only go down to around 6 K and 7 K, respectively. These results indicate that the large volumetric specific heat of Ag_2O shown in Fig. 3 originating from the optical phonon mode based on the phDOS (Fig. 4(b)) contributes to reach temperatures below 4.2 K. We

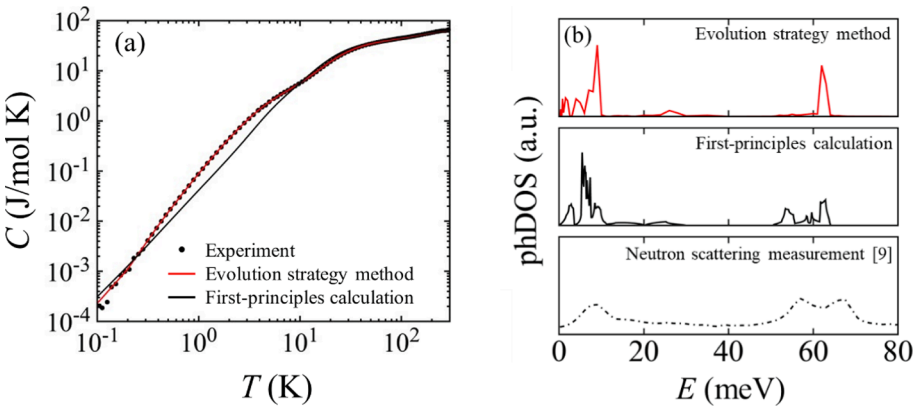

Fig. 4. (a) Experimental and calculated results of specific heat of Ag_2O in logarithmic form. Experimental results are represented by the black dots. The red solid line and black solid line represent fitted result by the ES method and calculated result by the first-principles calculation, respectively. (b) The phDOS calculated by the ES method shows similar peaks to that of calculated by first-principles calculation and inelastic neutron scattering measurement at 40 K [9]. (For interpretation of the references to colour in this figure legend, the reader is referred to the web version of this article.)

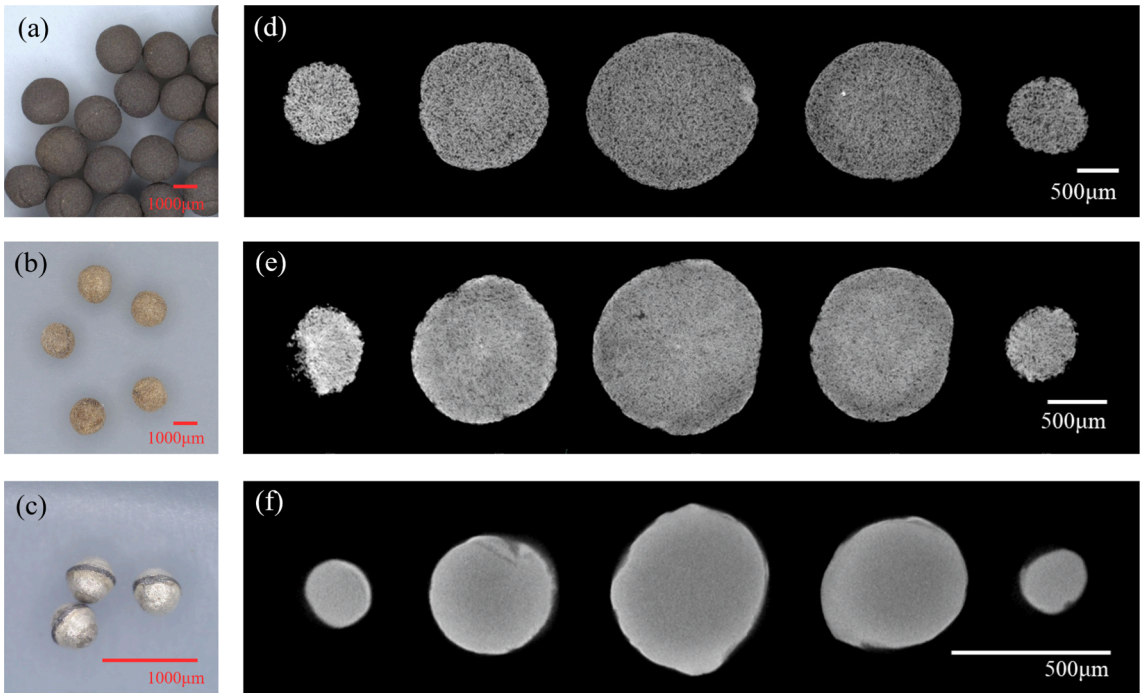

Fig. 5. (a)-(c) Photographs taken by optical microscopy. (a) Ag_2O spheres made by Sol-Gel technique, with a diameter of 2.0 mm and bulk density of ~ 25%. (b) Ag_2O spheres made by pseudo isotropic pressing technique, with a diameter of 1.5 mm and the bulk density of ~ 55%. (c) Ag_2O spheres made by the mold sintering technique, with a diameter of 0.5 mm and bulk density of 90% and above. (d)-(f) Series of images taken by the X-ray micro-CT, which display different degree of bulk density of the three spheres respectively.

also found that the cooling performance increases as the diameter of the particle decreases [30]. Smaller particle facilitates better heat exchange with He gas.

4. Summary

In this paper, the study covers both experimental and theoretical perspective of Ag_2O as a non-magnetic regenerator material with specific heat produced from "optical phonon degree of freedom". The specific heat of Ag_2O was measured and shows a non-Debye behavior at low temperatures, indicating optical phonon modes exist at low energy regions. At temperature below 10 K, the specific heat of Ag_2O is larger comparing to that of other two conventional regenerator materials, Pb and Bi, by the contribution of the optical phonon modes. To investigate the origin of the non-Debye behavior, both ES method and first-principles calculation were performed to calculate the phDOS. These results indicate that the phonon peaks around 10 meV contribute to the large specific heat of Ag_2O in cryogenic temperatures. Furthermore, we succeeded in applying a mold sintering technique to fabricate a Ag_2O particle of 0.5 mm in diameter and a density of more than 90%, which is practical to be used in regenerative cryocooler. The calculated cooling power of cryocooler using properties of the Ag_2O particle also shows that its lowest temperature can reach below 4.2 K. This feasibility study indicates that the concept to adopt a non-magnetic material with optical phonon degree of freedom as a regenerator material at cryogenic temperature can be realized.

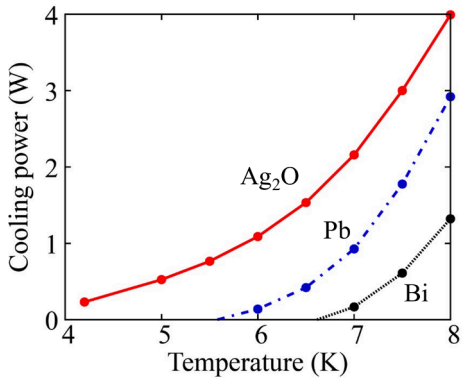

Fig. 6. Calculated cooling power of 2nd stage in GM cryocooler using regenerator materials Ag_2O, Pb, and Bi at different temperatures. The cooling power of cryocooler with Ag_2O remains even at 4.2 K.

CRediT authorship contribution statement

Sotaro Nishioka: Data curation, Formal analysis, Investigation, Methodology, Software, Visualization, Writing – original draft. **Shinji Masuyama:** Software, Writing – review & editing. **Akiko T. Saito:** Conceptualization, Investigation, Funding acquisition, Project administration, Supervision, Writing – review & editing.

Declaration of Competing Interest

The authors declare that they have no known competing financial interests or personal relationships that could have appeared to influence the work reported in this paper.

Data availability

The availability will be considered on a case-by-case basis.

Acknowledgement

The authors acknowledge Grants-in-Aid for Scientific Research from Japan Society for the Promotion of Science (JSPS KAKENHI Grant Number JP21H01267). We would like to extend our gratitude to Dr. T. Tadano for valuable advice on the calculation, and Dr. A. Kamimura for helping experiment. A special thanks to Dr. T. Hatano for the fruitful discussions. The calculations in this study were performed on the Numerical Materials Simulator at the NIMS.

References

[1] Sahashi M, Tokai Y, Kuriyama T, Nakagome H, Li R, Ogawa M, et al. Adv Cryog Eng 2009;35:1175–82. https://doi.org/10.1007/978-1-4613-0639-9_141.
[2] Kuriyama T, Hakamada R, Nakagome H, Tokai Y, Sahashi M, Li R, et al. Adv Cryog Eng 1990;35:1261–9. https://doi.org/10.1007/978-1-4613-0639-9_150.
[3] Okamura M, Sori N, Kuriyama T, Saito A, Sahashi M. Adv Cryog Eng 1996;42:415–22. https://doi.org/10.1007/978-1-4757-9059-7_55.
[4] Qiu LM, Numazawa T, Thummes G. Cryogenics 2001;41(9):693–6. https://doi.org/10.1016/S0011-2275(01)00146-1.
[5] Sato T, Numazawa T. Cryocoolers 2003;12:397–402. https://doi.org/10.1007/0-306-47919-2_52.
[6] Sata K, Yoshida T, Fujimoto S, Miyahara S, Kang YM. Supercond Sci Technol 1999;12:959–62. https://doi.org/10.1088/0953-2048/12/11/379.
[7] M. Endo, A. Saito, K. Harada, N. Tomimatsu, U.S. Patent, US 10,393,412 B2, 2019-08-27.
[8] Gupta MK, Mittal R, Chaplot SL, Rols S. J Appl Phys 2014;115:093507. https://doi.org/10.7567/JJAP.55.10TA09.
[9] T. Lan, C. W. Li, J. L. Niedziela, H. Smith, D. L. Abernathy, G. R. Rossman, and B. Fultz, Phys. Rev. B 2014,89:054306 (2014). Doi: 10.1103/PhysRevB.89.054306.
[10] L. V. Gregor and Kknneth S. Pitzer, J. Am. Chem. Soc. 1962,84,14:2664–2670. Doi: 10.1021/ja00873a003.
[11] Gupta MK, Mittal R, Rols S, Chaplot SL. Phys B 2012;407:2146–9. https://doi.org/10.1016/j.physb.2012.02.023.
[12] Assal J, Hallstedt B, Gauckler LJ. J Am Ceram Soc 1997;80(12):3054–60. https://doi.org/10.1111/j.1151-2916.1997.tb03232.x.
[13] Suzuki RO, Ogawa T, Ono K. J Am Ceram Soc 1999;82(8):2033–8. https://doi.org/10.1111/j.1151-2916.1999.tb02036.x.
[14] REGEN3.3 Package. National Institute of Standards and Technology, https://math.nist.gov/archive/regen/; 2009 [accessed 10 August 2023].
[15] Masuyama S, Fukuda Y, Imazu T, Numazawa T. Cryogenics 2011;51:337–40. https://doi.org/10.1016/j.cryogenics.2010.06.008.
[16] Giannozzi P, et al. J Phys Condens Matter 2009;21:395502. https://doi.org/10.1088/0953-8984/21/39/395502.
[17] Tadano T, Gohda Y, Tsuneyuki S. J Phys Condens Matter 2014;26:225402. https://doi.org/10.1088/0953-8984/26/22/225402.
[18] N. Hansen. and A. Ostermeier, Evolutionary Computation 2001,9,(2):159-195. Doi: 10.1162/106365601750190398.
[19] Perdew JP, Burke K, Ernzerhof M. Phys Rev Lett 1996;77:3865. https://doi.org/10.1103/PhysRevLett.77.3865.
[20] Hamann DR. Phys Rev B 2013;88:085117. https://doi.org/10.1103/PhysRevB.88.085117.
[21] Blöchl E. Phys Rev B 1994;50:17953. https://doi.org/10.1103/PhysRevB.50.17953.
[22] SSSP 1.2.1 Precision PBE: G. Prandini, A. Marrazzo, I. E. Castelli, N. Mounet and N. Marzari, npj Computational Materials 2018,4:72. Doi: 10.1038/s41524-018-0127-2.
[23] Schlipf M, Gygi F. Comp Phys Comm 2015;196:36. https://doi.org/10.1016/j.cpc.2015.05.011.
[24] E. Kucukbenli, M. Monni, B.I. Adetunji, X. Ge, G.A. Adebayo, N. Marzari, S. de Gironcoli, A. Dal Corso, arXiv:1404.3015. Doi: 10.48550/arXiv.1404.3015.
[25] Kennedy BJ, Kubota Y, Kato K. Solid State Commun 2005;136:177–80. https://doi.org/10.1016/j.ssc.2005.05.043.
[26] National Bureau of Standards, A Compendium of the Properties of Materials at Low Temperatures (Phase 1), In: V. J. Johnson (ed.), 4.142-3, United States:Wright Air Development Division; 1960.
[27] Cetas TC, Holste JC, Swenson CA. Phys Rev 1969;182(3):679. https://doi.org/10.1103/PhysRev.182.679.
[28] Musari AA, Joubert DP, Adebayo GA. Mater Res Express 2018;5:045704. https://doi.org/10.1088/2053-1591/aabd2a.
[29] Mittal R, Chaplot SL, Mishra SK, Bose PP. Phys Rev B 2007;75:174303. https://doi.org/10.1103/PhysRevB.75.174303.
[30] Nakagawa T, Miyauchi T, Shiraishi T, Shoda K, Yamamoto TA, Fujimoto Y, et al. Cryocoolers 2016;19:313–7.